ACS Partner Journal

CHEMICAL & BIOMEDICAL IMAGING

Open Access

pubs.acs.org/ChemBioImaging

Article

Live-Cell Imaging to Resolve Salt-Induced Liquid–Liquid Phase Separation of FUS Protein by Dye Self-Labeling

Yan Zhang,[#] Ning Xu,[#] Chunyu Yan, Xuelian Zhou, Qinglong Qiao, Lu Miao,* and Zhaochao Xu*

Cite This: *Chem. Biomed. Imaging* 2024, 2, 70–80

Read Online

ACCESS | Metrics & More | Article Recommendations | Supporting Information

ABSTRACT: The aggregation of fusion in sarcoma (FUS) in the cytoplasm and nucleus is a pathological feature of Amyotrophic lateral sclerosis (ALS) and Frontotemporal Dementia (FTD). Genetic mutations, abnormal protein synthesis, environmental stress, and aging have all been implicated as causative factors in this process. Salt ions are essential to many physiological processes in the body, and the imbalance of them is an important environmental stress factor in cells. However, their effect on liquid–liquid phase separation (LLPS) of FUS proteins in living cells is not well understood. Here, we map the various salt-induced LLPS of FUS in living cells by genetically coding and self-labeling FUS with organic dyes. The brightness and photostability of the dyes enable long-term imaging to track the mechanism of the assembly and disappearance of FUS phase separation. The FUS protein showed a better phase separation tendency under 0.3 M salt stimulation, and there was a large amount of FUS shuttling from the nucleus to the cytoplasm. At this concentration, various salt solutions displayed different effects on the phase separation of FUS protein, following the Hofmeister effects. We further observed that the assembly of FUS droplets underwent a process of rapid formation of small droplets, plateaus, and mutual fusion. Strikingly, The CsCl-stimulated FUS droplets were not completely reversible after washing, and some solid-like granules remained in the nucleus. Taken together, these results help broaden our understanding of the LLPS of FUS proteins in cellular stress responses.

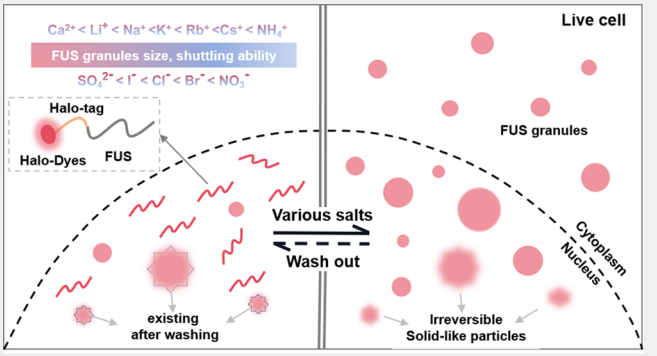

KEYWORDS: *FUS, LLPS, salt stress, Halo-tag, fluorescence imaging*

1. INTRODUCTION

The liquid–liquid phase separation process, usually mediated by weak polyvalent interactions of internally disordered proteins/regions, involves intracellular membrane-less organelles (MLOs), including germ (P) granules, stress granules, nucleolus, Cajal bodies, etc. These MLOs are highly dynamic and engage in frequent component exchange with the surrounding cytoplasm or nucleoplasm, performing specific biological functions.[1−3] However, the dysregulation of phase separation protein disturbs the normal function of cells by the accumulation of protein aggregates in the cytoplasm and nucleus, causing neurodegenerative diseases. Amyotrophic lateral sclerosis (ALS) and Frontotemporal Dementia (FTD) are typical neurodegenerative diseases whose pathogenesis is associated with FUS (fusion in sarcoma).[4,5] FUS is comprised of a N-terminal disordered region with low amino acid sequence complexity (LC), a segment with Arg-Gly-Gly motifs (RGG1, a folded RNA recognition domain), two additional RGG regions flanking a zinc-finger (ZnF) domain, and a C-terminal NLS sequence to locate FUS in the nucleus.[6] It can condense into droplets under diverse environmental stress such as pressure, pH, temperature, salt et al. Abnormal stress enables the destruction of the homeostasis of droplets and results in liquid-to-solid phase transition.[7,8] Therefore, a better study of the LLPS mechanism of FUS under different stress will not only help us to understand the function of MLOs but also to explore new prevention and treatment of related diseases.

Salts, such as cationic Li^+, Na^+, K^+, Rb^+, Cs^+, Ca^{2+}, and anionic Cl^-, I^-, SO_4^{2-} et al. are essential to many physiological processes in the body, and the imbalances of some salts have been reported to be associated with neurodegenerative diseases. For example, Li^+ was suggested to have neuroprotective effects against ALS.[9] K^+ and Na^+ play a major role in electric impulse conduction in excitable cells.[10,11] And Cl^- engages in the regulation of body fluids, preservation of electrical neutrality, acid–base balance, and muscular activity.[12] The imbalance of Na^+, K^+, and Cl^- ions in extracellular fluid caused the increase of osmotic pressure in intracellular

Received: September 3, 2023
Revised: September 29, 2023
Accepted: October 6, 2023
Published: October 23, 2023

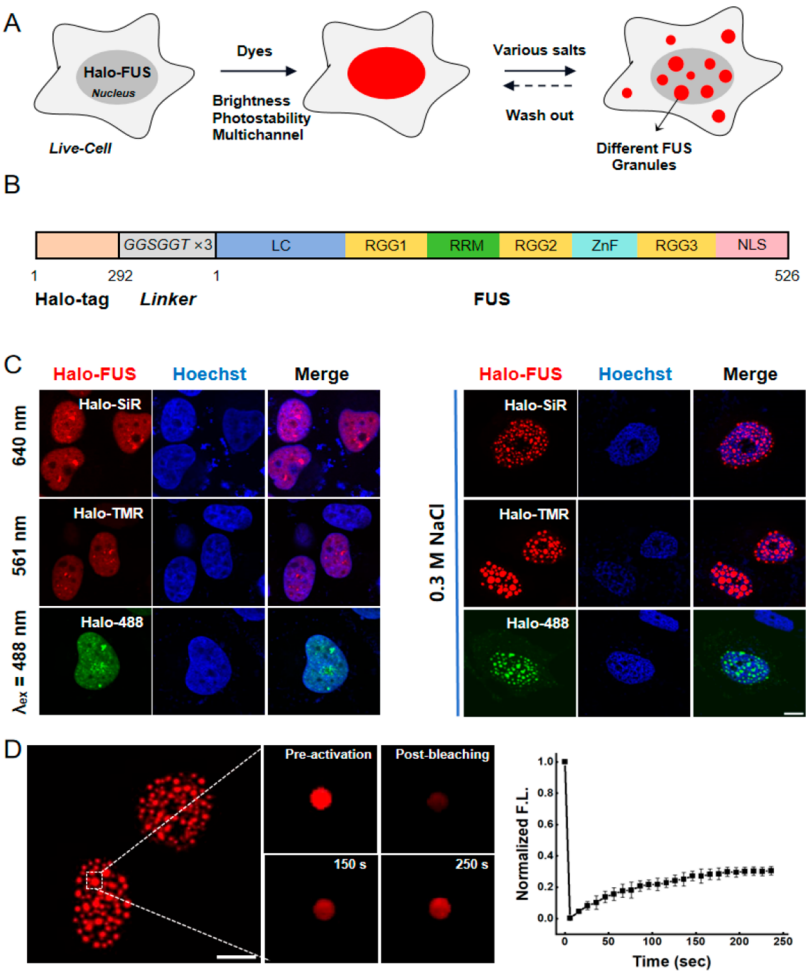

Figure 1. Studying of salt-induced LLPS of FUS in living cells. (A) Schematic of fluorescence imaging strategy for investigating salt-induced LLPS of FUS in living cells. (B) Construct of Halo-FUS fusion protein. (C) Fluorescence imaging of Halo-FUS protein labeled with different dyes before and after being induced by 0.3 M NaCl. For Halo-SiR, λ_{ex} = 640 nm; for Halo-TMR, λ_{ex} = 561 nm; for Halo-488, λ_{ex} = 488 nm. (D) FRAP recovery images and profiles of 0.3 M NaCl-induced Halo-FUS-TMR condensates. Scale bar = 10 μm. Data were shown as means ± SD with n = 3 individual droplet.

fluid and induced robust cytoplasmic translocation of FUS.[13,14] Importantly, some studies have found that alkali metals Li^+, Na^+, K^+, Rb^+, Cs^+ are distributed in different regions of the human brain, and highlight the potential role of the homeostasis deregulation of alkali metals in specific regions of the brain as a key factor in the pathogenesis of neurodegenerative diseases.[15] However, how these salts regulate the FUS protein LLPS is still poorly understood.

The mechanism through which salts interact with LLPS protein depends on the salt concentration. At a certain concentration of salt, the ions interact with the protein through salt-specific interactions known as Hofmeister effects.[16] Based on their ability to solubilize or precipitate proteins, salt ions are arranged into a series called the Hofmeister series.[17−19] Previous studies on FUS used the effects of different Hofmeister salts on their LLPS in vitro to gain insight into the relative strength of concentration-dependent intermolecular interactions. Murthy et al. found that the Hofmeister cations had little effect on LLPS of FUS LC domain, while phase separation of FUS LC followed the expected Hofmeister trend in the presence of the monovalent anions of the same ionic strength.[20] The in vitro experiment further found that the FUS proteins formed condensates at low salt concentrations, and they can reenter a phase-separated granule at high salt concentrations.[21] However, the cellular environment is complex and variable, and the effect of these salt ions on FUS phase separation in living cells was rarely reported.

Fluorescence labeling and live-cell tracking techniques enable dynamic visualization of protein function with high spatial and temporal resolution. Protein self-labeling tags (SNAP-tag, Halo-tag as commonly used ones) can singly link small molecule dyes to proteins of interest, which were widely used for live-cell protein imaging to monitor protein−protein or protein−molecule interaction, including single-virus visual tracking.[22−28] The biggest advantage of it is that various small molecule probes (brightness, photostability, color-tunable et al.) can be selected for different experiment requirements.[29−34]

In this paper, we investigated the LLPS dynamic of FUS protein under a variety of types and concentrations of salt solutions in the living cells (Figure 1A). By fusing protein self-labeling Halo-tag to FUS, small molecule dyes with brightness, photostability, and color-tunable properties were self-labeled to FUS for live-cell imaging its LLPS even by super-resolution microscopy. We found that the FUS protein showed a better phase separation tendency under 0.3 M salt stimulation, and there was a large amount of FUS shuttling from the nucleus to

https://doi.org/10.1021/cbmi.3c00094
Chem. Biomed. Imaging 2024, 2, 70−80

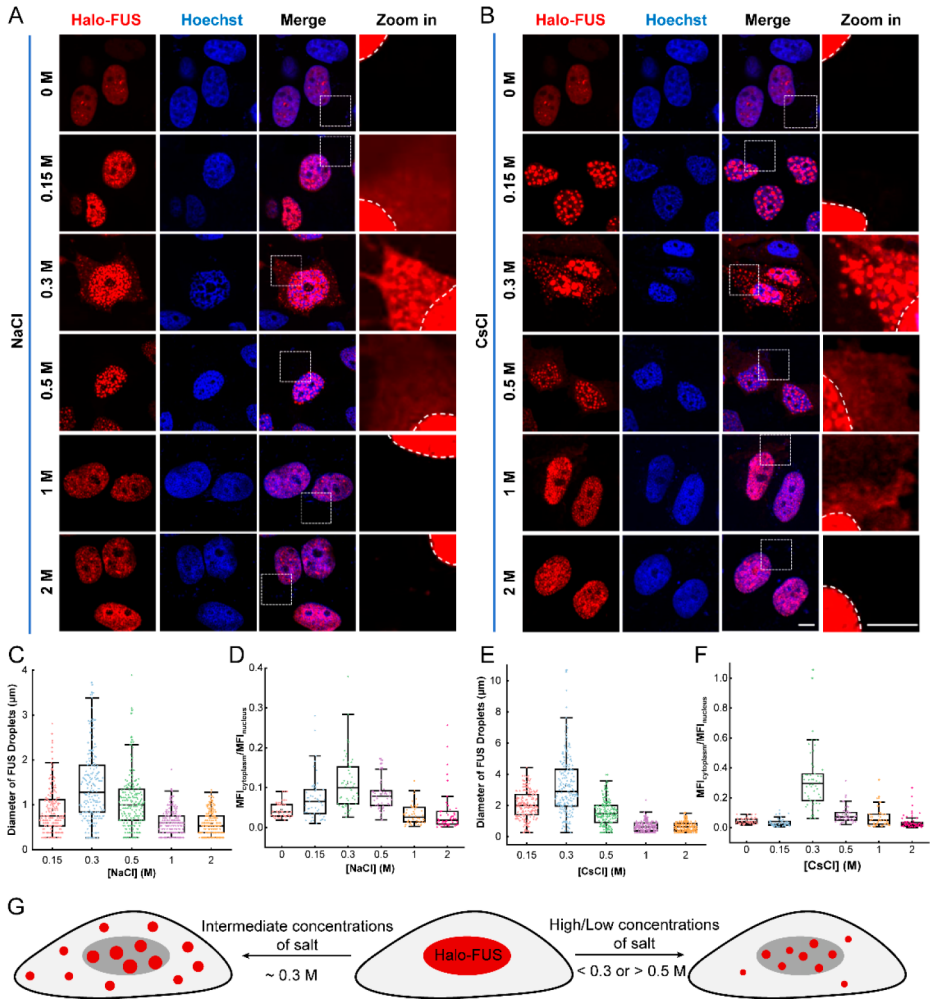

Figure 2. Live-cell imaging of Halo-FUS protein induced by different concentrations of NaCl and CsCl. (A, B) Representative fluorescence images of Halo-FUS granules induced by 0.15, 0.3, 0.5, 1, and 2 M NaCl (A) or CsCl (B) in the complete medium for 60 min. Hoechst 33342 was added for nuclear labeling. Scale bar = 10 μm. (C–F) Detailed statistics of imaging of A and B. (C, E) The diameter of FUS droplets after adding different concentrations of NaCl (C) and CsCl (E). n = 30–50 cells from three repeats. (D, F) The mean fluorescence intensity (MFI) ratio of Halo-FUS-TMR in the cytoplasm to the nucleus under the stimulation of different concentrations of NaCl (D) and CsCl (F). n = 50 cells from three repeats. (G) Schematic of Halo-FUS phase separation with different concentrations of salts.

the cytoplasm. At this concentration, various salt solutions show different effects on phase separation of FUS protein. Importantly, long-term structure illumination microscopy (SIM) imaging tracked the mechanism of the formation and disappearance of FUS phase separation after adding or washing out the salt. Not all phase separation granules were reversible, suggesting that salt stimulation may induce the transition of FUS proteins from the liquid to the solid phase, which gave us a deeper understanding of the phase separation characteristics of FUS in living cells under salt stress.

2. RESULTS AND DISCUSSION

2.1. Organic Dye Labeling of FUS Protein

Protein tag-based dye self-labeling strategies have genetically encoded and dye synthetic components, which combine protein site specificity and the flexibility of chemical reagents. It has been widely used in dynamic super-resolution fluorescence imaging of protein–protein interactions and subcellular structures. Here, we genetically encoded the Halo-tag to the N-terminal of FUS fully sequence, and three duplicate GGSGGT gene sequences were cloned as linkers between Halo and FUS, obtaining Halo-FUS fusion protein (Figure 1B). The selection of dyes needs to comprehensively consider biocompatibility, membrane permeability, brightness, and photostability to meet the requirement of super-resolution imaging on optical performance.

Dyes Halo-488, Halo-TMR, and Halo-SiR with different fluorescence channels (λ_{ex} = 488 nm, 561 nm, 640 nm) were selected to label the Halo-FUS protein, respectively, and hereinafter referred to as Halo-FUS-488, Halo-FUS-TMR, Halo-FUS-SiR. Confocal fluorescence imaging was used to visualize FUS in living cells and to assess whether fusion protein modifications affected its activity (Figure 1C). Colocalization imaging between Halo-FUS-dye and Hoechst 33342 (a commercial nuclear dye) on the nucleus was observed, proving the fluorescent labeling of the FUS protein. Moreover, after the addition of 0.3 M NaCl to the complete medium, we found that Halo-FUS lost the normal pattern and assembled into a large number of granules in the nucleus. In addition, there was no significant difference in droplet diameter and distribution of Halo-FUS labeled with different dyes (Figure S1A, B). To examine the dynamic properties of FUS granules, fluorescence recovery after photobleaching (FRAP)

https://doi.org/10.1021/cbmi.3c00094
Chem. Biomed. Imaging 2024, 2, 70–80

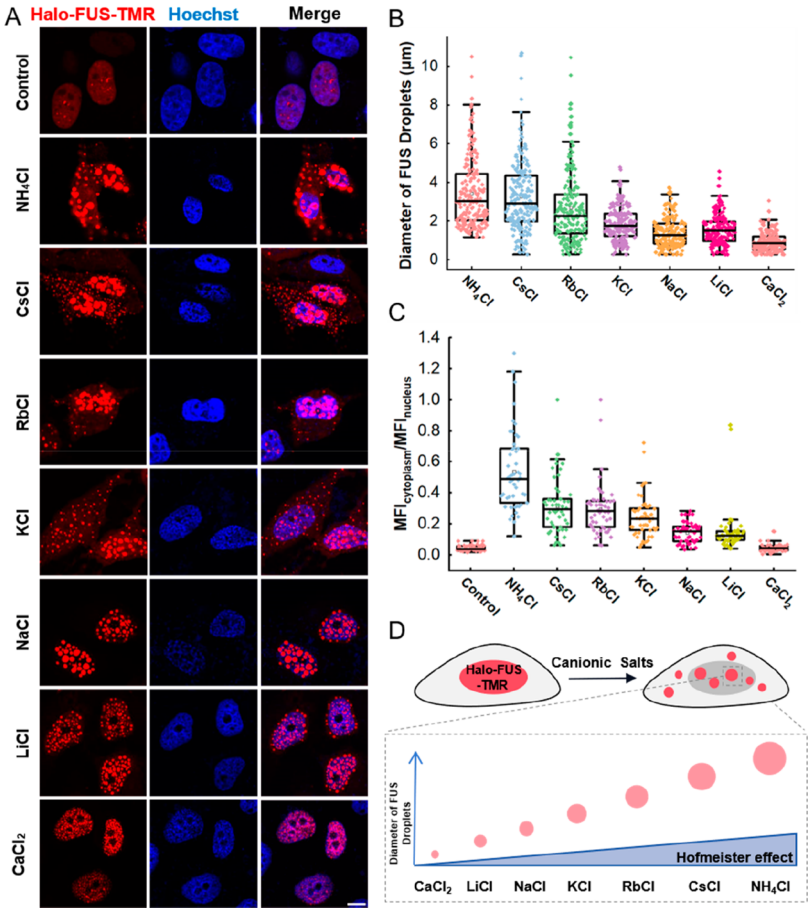

Figure 3. LLPS behavior of FUS induced by different cationic salts. (A) Fluorescence images of FUS granules induced by 0.3 M different cationic salts for 1 h. Hoechst 33342 was added for nuclear labeling. Scale bar = 10 μm. (B) Statistical data of the diameter of FUS droplets after adding different cationic salts. n = 30−50 cells from three repeats. (C) The MFI ratio of Halo-FUS-TMR in the cytoplasm to the nucleus under the stimulation of different types of cationic salts. n = 50 cells from three repeats. (D) Schematic of Halo-FUS phase separation with different Hofmeister series of cationic salts.

experiments were performed (Figure 1D, S1C, and S1D). The fluorescence recovery intensity of Halo-FUS-TMR granules reached ∼40% of the prebleaching fluorescence intensity in 250 s.

In addition, we found that during the FRAP experiment of Halo-FUS-488, after bleaching the fluorescence with a strong laser, the fluorescence was gradually bleached after a little recovery (Figure S1C). Perhaps because of the poor photostability of Halo-488, the fluorescence bleaching speed of Halo-488 was faster than the flow speed of Halo-FUS protein in the droplet. Meanwhile, Halo-SiR was difficult to be bleached with a strong laser because of its strong photostability (Figure S1D). It can be seen that different characteristics of fluorescent dyes have a great influence on the FRAP results of FUS proteins. In a follow-up experiment, we selected Halo-TMR dye to image FUS in order to compare the fluidity of proteins within the droplets.

2.2. Different Concentrations of Salt Induce Phase Separation of FUS in Living Cells

As reported, whether a system undergoes LLPS depends not only on the molecular identity and concentration but also on diverse environmental variables.[35] And the type and concentration of salts in the solution were one of the main influencing factors.[36] To better investigate LLPS of FUS in living cells under different salt concentrations, we transfected the Halo-FUS plasmids into HeLa cells and the cells were labeled by both Halo-TMR and Hoechst 33342 dyes.

0.15−2 M NaCl and CsCl were then added to the complete medium, respectively. The fluorescence imaging showed different phase separation phenomena (Figure 2). When stimulated by physiological salt concentration (0.15 M NaCl), a large number of FUS droplets were appeared and uniformly distributed in the nucleus. After zooming in and increasing the fluorescence contrast, the cytoplasm showed weak Halo-FUS fluorescence, but no droplets were observed (Figure 2A). With the doubling of NaCl concentration (0.3 M NaCl), the degree of FUS phase separation increased significantly, which was manifested as the increase in the diameter of FUS droplets in the nucleus, the enhancement of Halo-FUS mean fluorescence intensity (MFI) of cytoplasm, and the formation of obvious FUS droplets in the cytoplasm (Figure 2C, D). However, with the further increase of NaCl concentration, the size of FUS granules in the nucleus gradually decreased, and 1−2 M NaCl solution could no longer stimulate FUS proteins out of the nucleus. Meanwhile, similar results were obtained with different concentrations of CsCl (Figure 2B, E, F). The phase separation behavior of FUS was most obvious in the nucleus and cytoplasm under the stimulation of 0.3 M CsCl but decreased with the increase of CsCl concentration. Above all, intermediate salt concentrations (∼0.3 M) stimulated significant FUS phase separation

https://doi.org/10.1021/cbmi.3c00094
Chem. Biomed. Imaging 2024, 2, 70−80

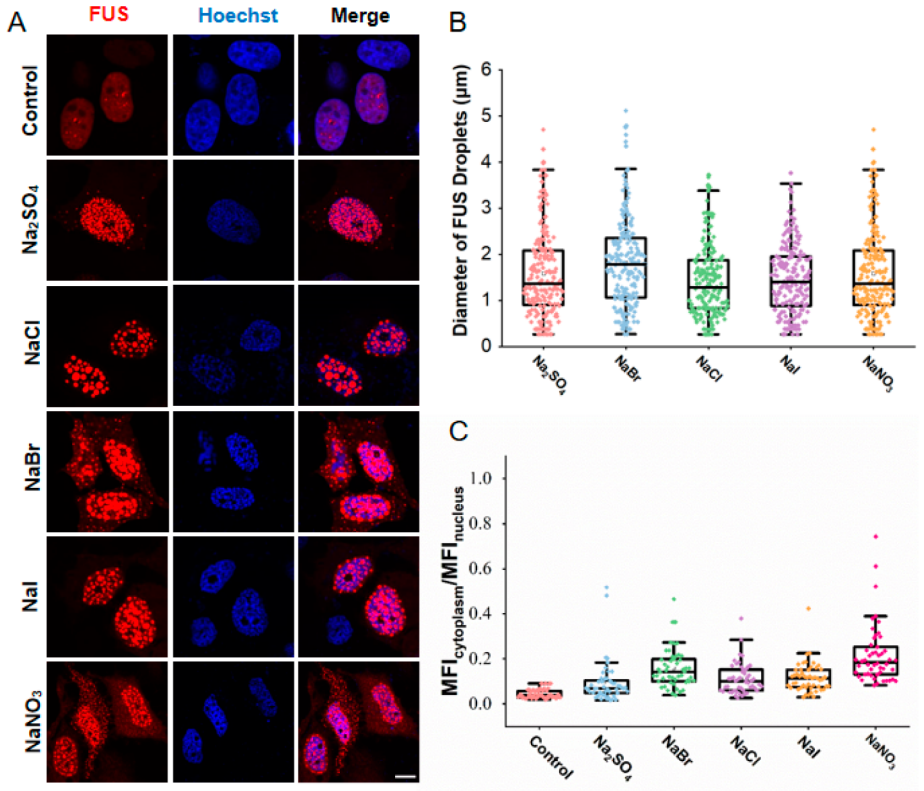

Figure 4. LLPS behavior of FUS induced by different anionic salts. (A) Fluorescence images of FUS granules induced by 0.3 M different anionic salts for 1 h. Hoechst 33342 was added for nuclear labeling. Scale bar = 10 μm. (B) Statistical data of the diameter of FUS droplets after adding different anionic salts. n = 30−50 cells from three repeats. (C) The MFI ratio of Halo-FUS-TMR in the cytoplasm to the nucleus under the stimulation of different anionic salts. n = 50 cells from three repeats.

behavior, while higher or lower salt concentrations induce weak or even no phase separation of FUS (Figure 2G). This result is consistent with partially salt-dependent in vitro phase separation studies, which increased in [NaCl] or [KCl] (up to 0.3 M) decreased or even eliminated phase separation.[37−39] The main reason may be that the salt with high concentration generates an osmotic pressure between monomers that prevents LLPS.[40] As known, nondiseased human brain has certain alkali metals level in different areas of the brain. For example, the highest levels of K, Rb, and Cs were found in the putamen. The highest levels of Na and Li were found in the frontal cortex and caudate nucleus. The homeostasis deregulation of alkali metals in specific brain regions as key factor in the pathogenesis of neurodegenerative diseases.[15] Our results show that 0.3 M of NaCl and CsCl induced the most pronounced FUS condensates, which is a potential concentration factor in the pathogenesis of ALS and FTD.

As reported, C-terminal NLS of FUS as a nuclear localization signal retains FUS in the nucleus via its interaction with the nuclear import receptors Transportin 1 and 2.[41] Here, we found that NaCl and CsCl could elicit FUS cytoplasmic redistribution in a certain concentration range (0.15−0.5 M for NaCl, 0.3−1 M for CsCl), of which 0.3 M was the strongest. It was demonstrated that the salt-stimulated cytoplasmic shuttling of FUS was dependent on the concentration of salt.[14] Currently, FUS cytoplasmic accumulation is observed in some ALS and FTD patients, and investigating stress conditions that can induce FUS nuclear export may help to understand its homeostasis mechanism.

In addition, the imbalance of ions (Na^+, K^+, et al.) in extracellular fluid was reported to cause the increase of osmotic pressure in intracellular fluid.[13] In order to investigate whether the differential FUS condensation is a result of ionic strength or osmotic pressure, we further examined the effects of two nonionic osmolytes: sucrose and sorbitol. As shown as Figure S2A, B, 0.15−0.5 M sucrose and sorbitol induced a large number of FUS droplets distributing uniformly in the nucleus. But there was little difference in the diameter of FUS droplets (Figure S2C) and MFI ratio of Halo-FUS-TMR in the cytoplasm to the nucleus (Figure S2D) under different concentrations of sucrose and sorbitol. It demonstrated that ionic strength is a key factor inducing differences in FUS droplet size and cytoplasmic shuttling.

2.3. Cation Salt Effects on the Phase Behavior of FUS

Hofmeister series ranks cations and anions according to their water affinity, from relatively large entropy of hydration and charge density (kosmotropes) to low entropy of hydration and low charge density (chaotropic). Kosmotropes are thought to be partially excluded from the protein backbone hydration layer on account of their strong hydration shell, while chaotropic can more easily shed their hydrating waters to partition to the protein backbone on account of their low entropy of hydration.[40] However, later studies have shown that such a rudimentary description fails to include all aspects of ion-specificity when another solute is present. Anomalies and reversals of the Hofmeister series have been observed in multiple systems, indicating a close interaction between the ion and the solute, which is related to the properties of the solute,

https://doi.org/10.1021/cbmi.3c00094
Chem. Biomed. Imaging 2024, 2, 70−80

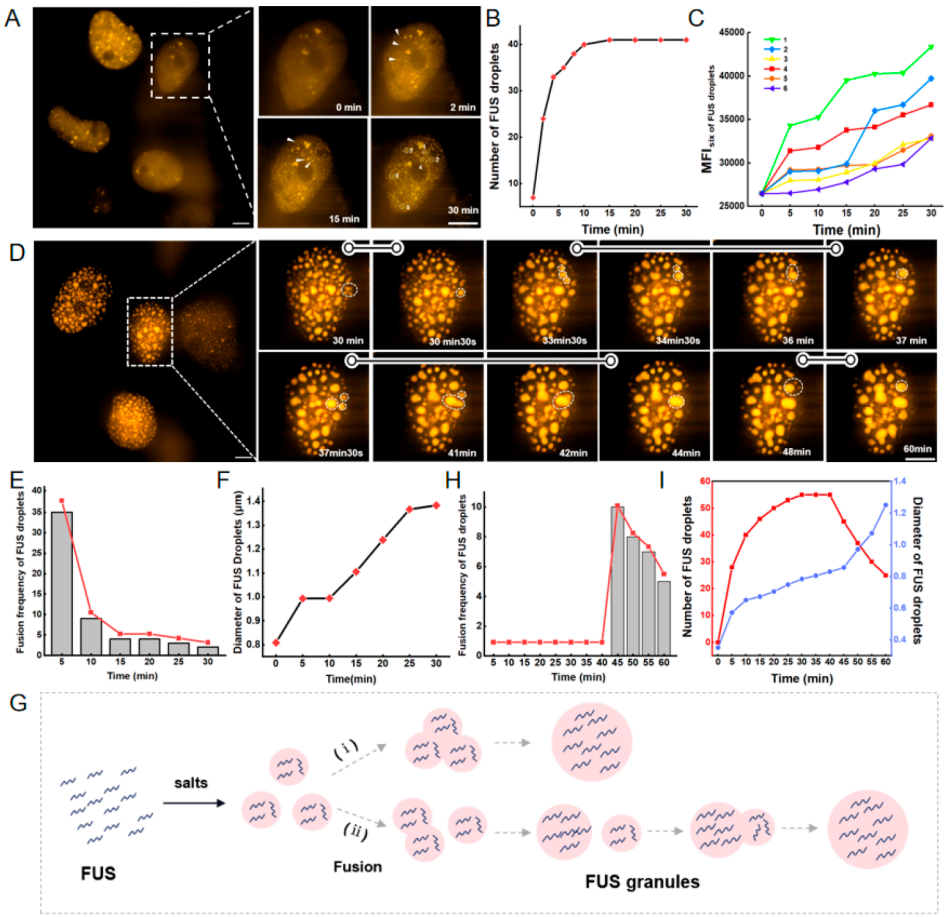

Figure 5. SIM tracking of the formation mechanism of FUS granules under salt stimulation. (A) SIM imaging of FUS granules formation within 30 min after the stimulation of 0.3 M CsCl. Imaging was performed immediately after the addition of CsCl. The time interval between each SIM image was 30 s with a course of 30 min. Scale bar = 5 μm. (B) The number of FUS granules formed every 5 min during the 30 min imaging process. (C) The MFI changes of six FUS granules in A, respectively. (D) SIM tracking of the fusion process of FUS granules within 30 min after 0.3 M CsCl stimulation. The cells were incubated with fresh medium containing 0.3 M CsCl for 30 min before imaging. Scale bar = 5 μm. (E) The fusion frequency of FUS granules per 5 min in D. (F) The changes of FUS granules diameter in D. (G) Schematic of the formation mechanism of salt-induced FUS granules in the living cells. (H) The fusion frequency of FUS granules per 5 min in Figure S6. (I) The changes in the number and diameter of FUS droplets are in Figure S6.

such as surface charge, polarity, softness, and heterogeneity.[42−44]

The cell is composed of many substances and its environment is complex and variable, here, we investigated the effect of different Hofmeister series of cation chloride salts on FUS phase separation in the living cells. NH_4Cl > CsCl > RbCl > KCl > NaCl > LiCl > $CaCl_2$ with from high (kosmotropes) to low (chaotropic) Hofmeister series were selected, using the concentration of 0.3 M was used to promote the obvious phase separation of FUS. Although this may not be the best concentration of all salts, it is more likely to judge the phase separation effect of salt-stimulated FUS by selecting the same concentration and maintaining the same conditions. As shown in Figure 3A, these ions can stimulate the FUS to form uniform phase separation particles in the nucleus. By statistical analysis of about 50 cells, it was found that ions with stronger Hofmeister effects were more likely to stimulate the FUS to produce larger granules (Figure 3B), as well as enter the cytoplasm to generate droplets (Figure 3C). $CaCl_2$ barely stimulated the FUS out of the nucleus. Our result displayed that FUS phase separation in the living cells followed the expected Hofmeister trend in the presence of the cations with the same ionic strength (Figure 3D). Ca^{2+} as the later salts in the Hofmeister series increased the solubility of FUS in solution by effectively weakening the strength of hydrophobic interactions, while the earlier salts NH_4^+ in the series strengthened hydrophobic interactions of FUS to form individually dispersed droplets. The strong hydrophobicity drove these droplets to fuse into much bigger granules. Therefore, the size of phase separation granules in living cells may be one of the criteria for evaluating FUS condensation level. This result is inconsistent with in vitro experiments, where the effects of Hofmeister cations following the series $Na^+ \sim K^+ > Rb^+ > Cs^+ > Li^+ \sim Ca^{2+}$ were shown for FUS protein.[21] We further examined the response of these cations to FUS^{P525L} (Figure S3). P525L is a disease-associated genetic mutant of FUS, which weakens the localization of the FUS in the nucleus, allowing it to enter the cytoplasm. The result showed that these ions encourage more FUS to enter the cytoplasm, and ions with stronger Hofmeister effects stimulate the FUS^{P525L} to produce larger granules. This is consistent with the results for wild-type FUS.

To detect the penetration of ions, we added the calcium probe Fluo-3 to the living cells to detect the calcium content. After adding calcium ions, the intracellular calcium ion concentration increased significantly, and the calcium ion

https://doi.org/10.1021/cbmi.3c00094
Chem. Biomed. Imaging 2024, 2, 70−80

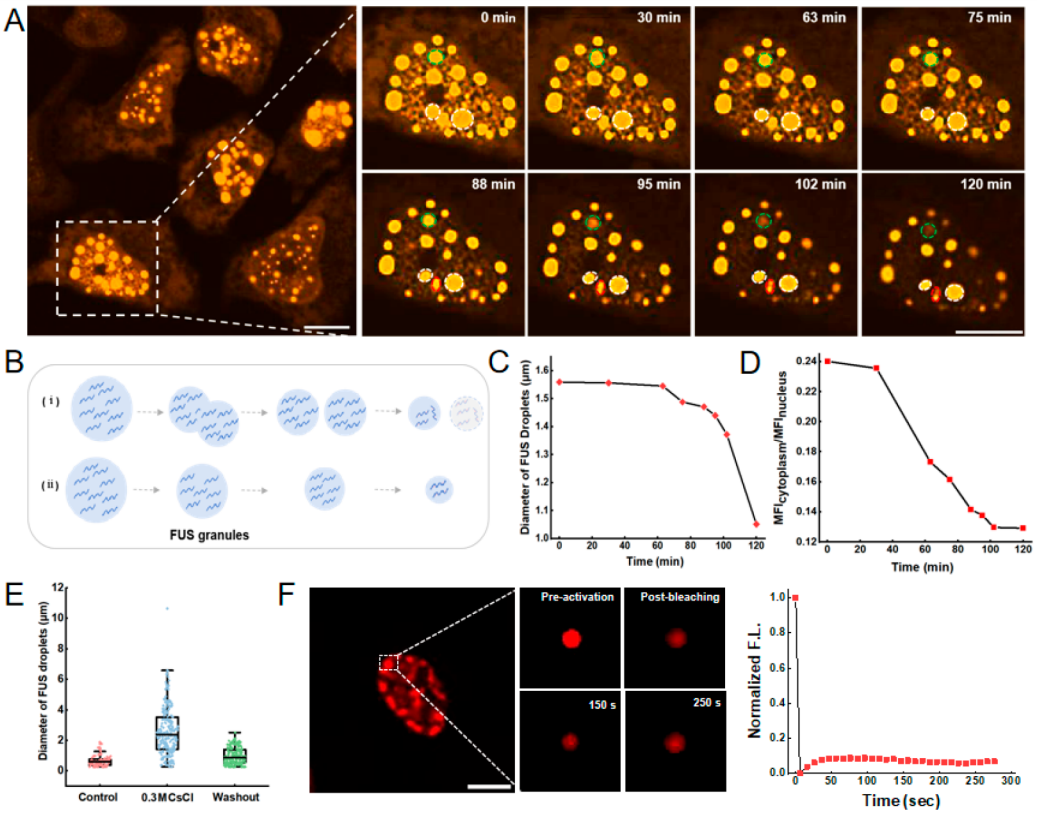

Figure 6. Reversibility analysis of salt-induced FUS granules after washing out the salt. (A) Fluorescence tracking of the disappearance process of salt-induced FUS granules after washing out the cells with fresh medium. The cells were incubated with fresh medium containing 0.3 M CsCl for 1 h and immediately imaged after replacing it with fresh medium without salt. The time interval between each fluorescence image was 30 s with a course of 30 min. Scale bar = 10 μm. (B) Schematic of FUS granules disappearance mechanism after removing salt. (C) The changes of FUS granules diameter in A. (D) The changes in MFI ratio of FUS in the cytoplasm to the nucleus. (E) Statistical data of the diameter of FUS droplets before and after washing out the salt. n = 30−40 cells from three repeats. (F) FRAP analysis of the FUS granules after washing out the salt.

concentration in the nucleus and cytoplasm was similar (Figure S4), which proved that calcium ions could penetrate into the cells. In addition, the stimulation of these cationic salts on FUS phase separation in living cells is not only due to the hydrophilicity of ions, but also other influencing factors, such as the effect of NH_4Cl on cell pH; excessive Ca^{2+} may cause mitochondrial dysfunctions, aberrant production of reactive oxygen species;[45] and even cell contraction caused by osmotic pressure to enlarge protein concentration.[14] In this paper, these ions were evaluated comprehensively in living cells and the possible rules were summarized.

2.4. Anionic Salt Effects on the Phase Behavior of FUS

We then further explored the effects of various anionic salts on FUS phase separation. Hofmeister series anionic salts SO_4^{2-} > Cl^- > Br^- > NO_3^- > I^- were used with the concentration of 0.3 M. Figure 4A showed that all five anionic salts induced phase separation of FUS proteins in the nucleus, and FUS droplets in the cytoplasm can be observed under the stimulation of $NaNO_3$ and NaBr. By statistical analysis of about 50 cells, it was found that the diameter of FUS droplets induced by NaBr anionic salts was slightly larger than that induced by other salts (Figure 4B). Meanwhile, all five anionic salts induced the FUS into the cytoplasm to generate droplets, but $NaNO_3$ and NaBr were relatively stronger than other salts (Figure 4C). In order of the capability of salt-induced FUS proteins to shuttle from the nucleus to the cytoplasm: NO_3^- > Br^- > Cl^- ~ I^- > SO_4^{2-}, which was inconsistent with the Hofmeister series.

Furthermore, we examined these anionic salts at the concentration of 0.15 M (Figure S5) and found that the order of anionic salts that induce FUS shuttling from nucleus to cytoplasm changed to SO_4^{2-} > NO_3^- > Br^- > Cl^- ~ I^-. It seemed that FUS protein was more easily induced to enter the cytoplasm from the nucleus than 0.3 M SO_4^{2-} at 0.15 M. This may be caused by the double negative charge and capacity for hydrogen bonding of SO_4^{2-}, which can act to screen positive charges, potentially complicating its influence on protein LLPS.

2.5. Dynamic LLPS of FUS Granules under Salt Stress

To explore the mechanism of salt-stimulated FUS formation, we tracked the formation process of FUS droplets in real time using structure illumination microscopy (SIM). First, real-time tracking was conducted for 0−30 min after the addition of 0.3 M CsCl. As shown in Figure 5A, before salt stimulation, FUS proteins were evenly distributed in the karyoplasm, with only a few amounts of coacervate droplets. After the addition of CsCl, a large number of tiny FUS droplets were rapidly produced in situ in the karyoplasm within 2 min. The number of tiny FUS droplets produced peaked at 10 min (Figure 5B), and remained constant for some time after that (10−30 min), with no fusion between the droplets. But during this time, the MFI in these droplets gradually increased, resulting in a higher signal-to-noise ratio to the background (Figure 5C), which

https://doi.org/10.1021/cbmi.3c00094
Chem. Biomed. Imaging 2024, 2, 70−80

may be due to the gradual absorption of scattered FUS proteins by the droplets. Furthermore, we tracked FUS droplets in the living cell for 30−60 min after salt stimulation, and the fusion processes among FUS droplets were observed (Figure 5D). According to the statistics, when the FUS droplets were small, the fusion frequency was relatively fast, with about 37 fusions occurring within 5 min. However, as the FUS droplets became larger due to fusion, the fusion frequency decreased, with only 2−4 fusions occurring every 5 min, where the fusion speed also slowed (Figure 5E, F). At the same time, the fusion between FUS droplets consists of two processes in which three droplets fuse or two droplets fuse (Figure 5G).

To confirm the above results, we tracked the whole process from formation to fusion of FUS droplets in the same cell (Figure S6). It was consistent with the previous fractional tracking results. The statistics in Figure 5H and I showed that a large number of FUS tiny droplets were generated rapidly after salt stimulation, reaching a plateau at 25−40 min, during which time the number of droplets remained unchanged and the average diameter of these droplets increased slightly. LLPS is an inherently metastable state. While the protein concentration within the protein-dense phase remains constant for a given condition, droplets do begin to grow in size. This growth results in part from Ostwald ripening: bigger droplets are more stable than smaller ones, resulting in the movement of protein out of smaller droplets into larger ones.[46] Then, when the tiny droplets reach a certain concentration and surface tension (the 40th minute), they begin to fuse with other droplets nearby, resulting in a decrease in the number of droplets, but a substantial increase in diameter.

Additionally, we also found that the assembly rate of FUS droplets was influenced by the initial protein expression level (Figure S7). Cells with higher FUS expression (cells with higher fluorescence intensity in the white box in Figure S7) formed FUS droplets in the nucleus more quickly than those with lower FUS expression (cells with lower fluorescence intensity in the red box in Figure S7) after the stimulation of salts, and the droplets in cells with higher FUS expression were larger in diameter. This result demonstrated that salt stress-induced protein phase separation is closely related to protein concentration. However, the assembly process of phase separation droplets was the same.

2.6. Reversibility Analysis of FUS Granules

To determine whether the FUS nuclear granules induced by salt stress were reversible, we first tracked the disassembly process of FUS granules induced by 0.3 M CsCl. After washing out the cells with a fresh medium, we took fluorescence imaging immediately. As shown in Figures 6A and B, the droplets in the nucleus gradually decrease and disappear in two ways: (i) most of the FUS droplets gradually shrank over time (droplets circled by the dashed white line), or even disappeared at last (droplets circled by the dashed red line); (ii) we also observed that the droplet splits into two small droplets, and then shrank further and disappeared (droplet circled by the dotted green line). The statistical data showed a gradual decrease in the diameter of FUS droplets in the nucleus, as well as the MFI ratio of FUS protein in the cytoplasm to the nucleus (Figure 6C, D), indicating that the FUS protein in the cytoplasm was shuttled back into the nucleus.

We further investigated the reversibility of salt stimulation of cells by counting the diameter changes of FUS droplets in 30−40 cells. The FUS phase separation phenomenon recovered in 90% of cells after washing, but a small number of cells did not return to the initial state (Figure 6E, S8). Figure 6F displayed a cell still in a phase separation state in the nucleus after washing by fresh medium for 2 h, and the FRAP experiment showed that the phase separation granules had only weak fluorescence recovery after photobleaching, indicating that the fluidity of the FUS protein in the granules was very poor. The results showed that CsCl incubation for 1 h could destroy the homeostasis of FUS droplet, which may lead to the transition from liquid phase to solid phase. In actuality, a solid-like state has been considered the final stage of LLPS maturation as a general phenomenon, and the temporal comparison is key to assessing droplet maturation. An in vitro study has shown that full-length FUS proteins lose their liquid-like properties for at least 8 h. Here, CsCl drove some of the FUS droplets to mature into the solid phase within 1 h. We propose that liquid-like compartments carry the trade-off between functionality and risk of aggregation, and salt stimulation may tip the balance and accelerate aggregation, which is a potential risk factor for neurodegenerative diseases.

3. CONCLUSION

We have developed a live-cell visualization strategy to resolve the phase separation of FUS by fusing the Halo protein tag to the N-terminal of FUS. Halo-488, Halo-TMR, and Halo-SiR can be labeled separately from Halo-FUS for imaging in different fluorescence channels. We first investigated the effect of salt concentration and type on FUS phase separation and found that intermediate [salt] (~0.3 M) stimulated significant FUS phase separation behavior, and the FUS protein shuttled to the cytoplasm to form obvious droplets. However, higher or lower salt concentrations induce weak or even no phase separation of FUS. Then, according to the size of the FUS droplets and the ability of FUS cytoplasmic shuttling after salt stimulation, we evaluated the effects of different cationic salts and anionic salts on FUS phase separation, and the cation order was obtained as NH_4Cl > CsCl > RbCl > KCl > NaCl > LiCl > $CaCl_2$, consistent with its Hofmeister sequence, and the anion order was NO_3^- > Br^- > Cl^- ~ I^- > SO_4^{2-}. Furthermore, with the help of the diffraction-limited spatial resolution and the excellent dynamic imaging performance of SIM, the details of the assembly and disappearance of FUS phase separation were discovered. The assembly of FUS droplets went through small droplets forming, plateauing, and merging into larger droplets. We also observed for the first time the droplets splitting and then disappearing after washing the cells. Notably, CsCl-stimulated FUS droplets did not fully return to the initial state after washing, but may form solid-like granules in the nucleus, indicating the potential impact of salt stimulation on neurodegenerative diseases.

4. MATERIALS AND METHODS

4.1. Materials

Taq Plus DNA Polymerase, dNTP 10 mM Mixture, dN(U)TP 25 mM Mixture, T7 RNA Polymerase, Urea, Acrylamide, Acryl/Bis 30% Solution (29:1), Water-DEPC Treated Water, RNase-free double-distilled water (ddH_2O) were obtained from Sangon Biotech. Restriction enzyme was purchased from Takara. Hieff Clone Plus Multi One Step Cloning Kit, MolPure PCR Purification Kit, MolPure Gel Extraction Kit, and MolPure Plasmid Mini Kit were bought from Yeasen. Sodium chloride, potassium chloride, sodium nitrate, and calcium chloride were purchased from Kermel. Cesium chloride,

https://doi.org/10.1021/cbmi.3c00094
Chem. Biomed. Imaging 2024, 2, 70−80

rubidium chloride, and anhydrous lithium chloride were purchased from Macklin. Sodium iodide, sodium bromide, and sodium sulfate were purchased from Aladdin. Unless otherwise specifically stated, all reagents were used without further treatment or purification.

4.2. Plasmid and Constructs

The Halo fragment was obtained by PCR amplification with primers 5′-GGCCGCCACCAAGCTTGATATCGCCACCATGGCAGAAATCGGTACTGGCTTT-3′ and 5′-TGATCCTCCTGTTCCGCCAGATCCACCGGATCCCGTCGACAGCCAGCGCG-3′. Similarly, primers 5′-TGGCGGAACAGGAGGATCAGGAGGTACCGGTGCTCCGGCGGTACTATGGCCTCAAACGATTATACCC-3′ and 5′-GAATTCGGCGGCCGCTCTAGATTAATACGGCCTCTCCCTGC-3′ were used for PCR amplification to obtain FUS fragments. The vectors carrying the two fragments were double-digested with restriction enzymes (*Bam*HI and EcoRV). Finally, the two fragments were connected to the vector through the Hieff Clone Plus Multi One Step Cloning Kit (Yeasen) to construct pDNA3.1-Halo-FUS plasmid.

4.3. Plasmid Transfection

10^4 HeLa cells (ATCC CCL-2) were seeded into each glass bottom cell culture dish (35 mm, Nest). The cells were then transfected with 500 ng pDNA3.1-Halo-FUS vector using 1.5 μL Lipofectamine 3000 per dish. The phase separation experiment of postrelated FUS was performed 48 h after transfection.

4.4. Dye Labeling and Live Cell Imaging

For FUS protein imaging in living HeLa cells, the cells transfected with the pDNA3.1-Halo-FUS plasmid were incubated with fresh medium containing Halo-dyes (500 nM Halo-SiR, 500 nM Halo-TMR, or 1 μM Halo-488) and 1 μM Hoechst 33342. After incubation at 37 °C in the presence of 5% CO_2 for 1 h, fluorescence imaging was performed using the 100 × oil drop objective of the OLYMPUS laser scanning confocal microscope after being washed three times with fresh medium. For Halo-SiR, λ_{ex} = 640 nm; for Halo-TMR, λ_{ex} = 561 nm; for Halo-488, λ_{ex} = 488 nm.

4.5. Fluorescence Recovery after Photobleaching (FRAP)

HeLa cells expressing Halo-FUS were treated with 0.3 M NaCl solution to form stress granules, and the granules were measured by FRAP in the OLYMPUS confocal system by bleaching mode. In short, the protein particle region was selected with a circular pattern, and each granule was bleached with a 488 nm laser at 100% power for about 10 s. The delay imaging interval was set to 30 s for 5 min.

4.6. Fluorescence Imaging of Various Salt-Induced FUS LLPS

To prevent cell contamination, different types (NH_4Cl, CsCl, RbCl, LiCl, KCl, NaCl, $CaCl_2$, Na_2SO_4, NaBr, NaI, and $NaNO_3$) or concentrations (0.15, 0.3, 0.5, 1, and 2 M) of salt solutions were prepared in a sterile environment. Different concentrations of salt solution were prepared according to the experimental requirements, and all reagents were dissolved in a DMEM medium. Dye labeling was performed before adding different salt solutions, and then the cells were incubated with fresh medium containing different types or concentrations of salt solutions at 37 °C and 5% CO_2 for 1 h after cleaning three times. Fluorescence imaging was performed using an OLYMPUS laser scanning confocal microscope.

4.7. SIM Imaging for FUS Dynamic Tracking

To track the dynamic process of phase separation of FUS by SIM imaging, HeLa cells were incubated with fresh medium containing 500 nM Halo-TMR and 1 μM Hoechst 33342 at 37 °C in 5% CO_2 for 1 h. The cell position was confirmed under a microscope, and the final concentration of 0.3 M CsCl was added in situ and immediately imaged.

To track the dynamic process of phase separation and fusion of FUS by SIM imaging, HeLa cells were incubated with fresh medium containing 500 nM Halo-TMR and 1 μM Hoechst 33342 at 37 °C and 5% CO_2 for 1 h and washed three times with fresh medium. HeLa cells were incubated with a medium containing 0.3 M CsCl at 37 °C and 5% CO_2 for 30 min, and then immediately imaged.

Fluorescence imaging was performed using a N-SIM super-resolution microscope. The microscope was purchased from Nikon and imaged in SIM-3D. Recordable moire fringes are generated by irradiating the subresolution structure in the sample with high spatial frequency laser interference fringes. These more fringes include the modulation information on the subresolution structure of the sample.

4.8. Fluorescence Imaging for FUS Particle Reversibility Analysis

To analyze the reversibility of FUS particles by fluorescence imaging, HeLa cells were incubated with fresh medium containing 500 nM Halo-TMR and 1 μM Hoechst 33342 staining at 37 °C and 5% CO_2 for 1 h, and washed three times with fresh medium. HeLa cells were incubated with a medium containing 0.3 M CsCl at 37 °C and 5% CO_2 for 60 min, and then replaced with fresh medium for immediate imaging.

4.9. Quantification and Statistical Analysis

To evaluate the location information on particles after salt-induced FUS protein phase separation in living cells, ImageJ was used to obtain the mean fluorescence intensity ($MFI_{nucleus}$, $MFI_{cytoplasm}$) of the cytoplasm and nucleus of random 50 cells, and randomly depicted background fluorescence (MFI_{bg}) was collected. The relative position of the FUS phase-separated particles in the cell ($MFI_{cytoplasm}/MFI_{nucleus}$) is obtained according to the following formula:

$$MFI_{cytoplasm}/MFI_{nucleus} = \frac{MFI_{cytoplasm} - MFI_{bg}}{MFI_{nucleus} - MFI_{bg}}$$

ImageJ was used to calculate the area of FUS particles to obtain the particle size information on the droplet particles, and the particle size information on 200 random FUS droplets was obtained. Statistical analysis is performed in Origin or Microsoft Excel. The imaging images were converted to TIFF images using ImageJ. Brightness and contrast are adjusted in Adobe Photoshop, and usually, the same adjustments are applied to all conditions in the figure at the appropriate time.

■ ASSOCIATED CONTENT

Supporting Information

The Supporting Information is available free of charge at https://pubs.acs.org/doi/10.1021/cbmi.3c00094.

The LLPS behavior of FUS induced by different anionic salts, Fluorescence imaging tracked the formation mechanism of FUS particles under salt stimulation, SIM imaging of FUS granules formation after the stimulation of 0.3 M CsCl, Fluorescence imaging of salt-induced FUS granules after washing out the salt (PDF)

■ AUTHOR INFORMATION

Corresponding Authors

Lu Miao − *CAS Key Laboratory of Separation Science for Analytical Chemistry, Dalian Institute of Chemical Physics, Chinese Academy of Sciences, Dalian 116023, China*; Email: miaolu@dicp.ac.cn

Zhaochao Xu − *School of Chemistry, Dalian University of Technology, Dalian 116024, China; CAS Key Laboratory of Separation Science for Analytical Chemistry, Dalian Institute of Chemical Physics, Chinese Academy of Sciences, Dalian 116023, China*; orcid.org/0000-0002-2491-8938; Email: zcxu@dicp.ac.cn

https://doi.org/10.1021/cbmi.3c00094
Chem. Biomed. Imaging 2024, 2, 70−80

Authors

Yan Zhang − *School of Chemistry, Dalian University of Technology, Dalian 116024, China; CAS Key Laboratory of Separation Science for Analytical Chemistry, Dalian Institute of Chemical Physics, Chinese Academy of Sciences, Dalian 116023, China*

Ning Xu − *School of Chemistry, Dalian University of Technology, Dalian 116024, China; CAS Key Laboratory of Separation Science for Analytical Chemistry, Dalian Institute of Chemical Physics, Chinese Academy of Sciences, Dalian 116023, China*

Chunyu Yan − *School of Chemistry, Dalian University of Technology, Dalian 116024, China; CAS Key Laboratory of Separation Science for Analytical Chemistry, Dalian Institute of Chemical Physics, Chinese Academy of Sciences, Dalian 116023, China*

Xuelian Zhou − *School of Chemistry, Dalian University of Technology, Dalian 116024, China; CAS Key Laboratory of Separation Science for Analytical Chemistry, Dalian Institute of Chemical Physics, Chinese Academy of Sciences, Dalian 116023, China*

Qinglong Qiao − *CAS Key Laboratory of Separation Science for Analytical Chemistry, Dalian Institute of Chemical Physics, Chinese Academy of Sciences, Dalian 116023, China*

Complete contact information is available at: https://pubs.acs.org/10.1021/cbmi.3c00094

Author Contributions

#Y.Z. and N.X. are co-first authors.

Notes

The authors declare no competing financial interest.

■ ACKNOWLEDGMENTS

We are grateful for the financial support from the National Natural Science Foundation of China (22378385, 22225806, 22078314, 22278394), Dalian Institute of Chemical Physics (DICP I202142, DICPI202227).

■ REFERENCES

(1) Banani, S. F.; Lee, H. O.; Hyman, A. A.; Rosen, M. K. Biomolecular condensates: organizers of cellular biochemistry. *Nat. Rev. Mol. Cell Biol.* **2017**, *18*, 285−298.

(2) Lyon, A. S.; Peeples, W. B.; Rosen, M. K. A framework for understanding the functions of biomolecular condensates across scales. *Nat. Rev. Mol. Cell Biol.* **2021**, *22*, 215−235.

(3) Wang, B.; Zhang, L.; Dai, T.; Qin, Z.; Lu, H.; Zhang, L.; Zhou, F. Liquid-liquid phase separation in human health and diseases. *Signal Transduct. Target Ther.* **2021**, *6*, 290.

(4) Patel, A.; Lee, H. O.; Jawerth, L.; Maharana, S.; Jahnel, M.; Hein, M. Y.; Stoynov, S.; Mahamid, J.; Saha, S.; Franzmann, T. M.; Pozniakovski, A.; Poser, I.; Maghelli, N.; Royer, L. A.; Weigert, M.; Myers, E. W.; Grill, S.; Drechsel, D.; Hyman, A. A.; Alberti, S. A Liquid-to-Solid Phase Transition of the ALS Protein FUS Accelerated by Disease Mutation. *Cell* **2015**, *162*, 1066−1077.

(5) Murray, D. T.; Kato, M.; Lin, Y.; Thurber, K. R.; Hung, I.; McKnight, S. L.; Tycko, R. Structure of FUS Protein Fibrils and Its Relevance to Self-Assembly and Phase Separation of Low-Complexity Domains. *Cell* **2017**, *171*, 615−627.

(6) Ederle, H.; Dormann, D. TDP-43 and FUS en route from the nucleus to the cytoplasm. *FEBS Lett.* **2017**, *591*, 1489−1507.

(7) Kitahara, R.; Yamazaki, R.; Ide, F.; Li, S.; Shiramasa, Y.; Sasahara, N.; Yoshizawa, T. Pressure-Jump Kinetics of Liquid-Liquid Phase Separation: Comparison of Two Different Condensed Phases of the RNA-Binding Protein, Fused in Sarcoma. *J. Am. Chem. Soc.* **2021**, *143*, 19697−19702.

(8) Krainer, G.; Welsh, T. J.; Joseph, J. A.; Espinosa, J. R.; Wittmann, S.; de Csillery, E.; Sridhar, A.; Toprakcioglu, Z.; Gudiskyte, G.; Czekalska, M. A.; Arter, W. E.; Guillen-Boixet, J.; Franzmann, T. M.; Qamar, S.; St George-Hyslop, P.; Hyman, A. A.; Collepardo-Guevara, R.; Alberti, S.; Knowles, T. P. J. Reentrant liquid condensate phase of proteins is stabilized by hydrophobic and non-ionic interactions. *Nat. Commun.* **2021**, *12*, 1085.

(9) Forlenza, O. V.; De-Paula, V. J.; Diniz, B. S. Neuroprotective effects of lithium: implications for the treatment of Alzheimer's disease and related neurodegenerative disorders. *ACS Chem. Neurosci.* **2014**, *5*, 443−450.

(10) Michell, A. R. Sodium: Physiology. In *Encyclopedia of Human Nutrition*, 3rd ed.; Caballero, B., Ed.; Academic Press: Waltham, 2013; Vol. *4*, pp 200−203.

(11) Appel, L. J. Potassium. In *Encyclopedia of Human Nutrition*, 3rd ed.; Caballero, B., Ed.; Academic Press: Waltham, 2013; Vol. *4*, pp 52−55.

(12) Fries, M. R.; Conzelmann, N. F.; Gunter, L.; Matsarskaia, O.; Skoda, M. W. A.; Jacobs, R. M. J.; Zhang, F.; Schreiber, F. Bulk Phase Behavior vs Interface Adsorption: Specific Multivalent Cation and Anion Effects on BSA Interactions. *Langmuir* **2021**, *37*, 139−150.

(13) Hock, E. M.; Maniecka, Z.; Hruska-Plochan, M.; Reber, S.; Laferriere, F.; Sahadevan, M. K. S.; Ederle, H.; Gittings, L.; Pelkmans, L.; Dupuis, L.; Lashley, T.; Ruepp, M. D.; Dormann, D.; Polymenidou, M. Hypertonic Stress Causes Cytoplasmic Translocation of Neuronal, but Not Astrocytic, FUS due to Impaired Transportin Function. *Cell Rep.* **2018**, *24*, 987−1000.

(14) Gao, C.; Gu, J.; Zhang, H.; Jiang, K.; Tang, L.; Liu, R.; Zhang, L.; Zhang, P.; Liu, C.; Dai, B.; Song, J. Hyperosmotic-stress-induced liquid-liquid phase separation of ALS-related proteins in the nucleus. *Cell Rep* **2022**, *40*, 111086.

(15) Ramos, P.; Santos, A.; Pinto, E.; Pinto, N. R.; Mendes, R.; Magalhães, T.; Almeida, A. Alkali metals levels in the human brain tissue: Anatomical region differences and age-related changes. *Journal of Trace Elements in Medicine and Biology* **2016**, *38*, 174−182.

(16) Zhang, Y.; Cremer, P. S. Chemistry of Hofmeister anions and osmolytes. *Annu. Rev. Phys. Chem.* **2010**, *61*, 63−83.

(17) Lyon, A. S.; Peeples, W. B.; Rosen, M. K. A framework for understanding the functions of biomolecular condensates across scales. *Nat. Rev. Mol. Cell Biol.* **2021**, *22*, 215−235.

(18) Maity, H.; Baidya, L.; Reddy, G. Salt-induced transitions in the Conformational Ensembles of Intrinsically Disordered Proteins. *J. Phys. Chem. B* **2022**, *126*, 5959−5971.

(19) Otis, J. B.; Sharpe, S. Sequence Context and Complex Hofmeister Salt Interactions Dictate Phase Separation Propensity of Resilin-like Polypeptides. *Biomacromolecules* **2022**, *23*, 5225−5238.

(20) Murthy, A. C.; Dignon, G. L.; Kan, Y.; Zerze, G. H.; Parekh, S. H.; Mittal, J.; Fawzi, N. L. Molecular interactions underlying liquid-liquid phase separation of the FUS low-complexity domain. *Nat. Struct Mol. Biol.* **2019**, *26*, 637−648.

(21) Krainer, G.; Welsh, T. J.; Joseph, J. A.; Espinosa, J. R.; Wittmann, S.; de Csilléry, E.; Sridhar, A.; Toprakcioglu, Z.; Gudiškytė, G.; Czekalska, M. A.; Arter, W. E.; Guillén-Boixet, J.; Franzmann, T. M.; Qamar, S.; George-Hyslop, P. S.; Hyman, A. A.; Collepardo-Guevara, R.; Alberti, S.; Knowles, T. P. J. Reentrant liquid condensate phase of proteins is stabilized by hydrophobic and non-ionic interactions. *Nat. Commun.* **2021**, *12*, 1085.

(22) Gautier, A.; Juillerat, A.; Heinis, C.; Correa, I. R., Jr.; Kindermann, M.; Beaufils, F.; Johnsson, K. An engineered protein tag for multiprotein labeling in living cells. *Chem. Biol.* **2008**, *15*, 128−136.

(23) Los, G. V.; Encell, L. P.; McDougall, M. G.; Hartzell, D. D.; Karassina, N.; Zimprich, C.; Wood, M. G.; Learish, R.; Ohana, R. F.; Urh, M.; Simpson, D.; Mendez, J.; Zimmerman, K.; Otto, P.; Vidugiris, G.; Zhu, J.; Darzins, A.; Klaubert, D. H.; Bulleit, R. F.; Wood, K. V. HaloTag: a novel protein labeling technology for cell imaging and protein analysis. *ACS Chem. Biol.* **2008**, *3*, 373−382.

(24) Leng, S.; Qiao, Q.; Miao, L.; Deng, W.; Cui, J.; Xu, Z. A wash-free SNAP-tag fluorogenic probe based on the additive effects of quencher release and environmental sensitivity. *Chem. Commun.* **2017**, *53*, 6448−6451.
(25) Qiao, Q.; Liu, W.; Chen, J.; Zhou, W.; Yin, W.; Miao, L.; Cui, J.; Xu, Z. A naphthalimide-derived fluorogenic probe for SNAP-tag with a fast record labeling rate. *Dyes Pigm.* **2017**, *147*, 327−333.
(26) Liu, S. L.; Wang, Z. G.; Xie, H. Y.; Liu, A. A.; Lamb, D. C.; Pang, D. W. Single-Virus Tracking: From Imaging Methodologies to Virological Applications. *Chem. Rev.* **2020**, *120*, 1936−1979.
(27) Liu, A. A.; Zhang, Z.; Sun, E. Z.; Zheng, Z.; Zhang, Z. L.; Hu, Q.; Wang, H.; Pang, D. W. Simultaneous Visualization of Parental and Progeny Viruses by a Capsid-Specific HaloTag Labeling Strategy. *ACS Nano* **2016**, *10*, 1147−1155.
(28) Miao, L.; Zhou, W.; Yan, C.; Zhang, Y.; Qiao, Q.; Zhou, X.; Chen, Y.; Wang, G.; Guo, Z.; Liu, J.; Piao, H.; Pan, X.; Yan, M.; Zhao, W.; Li, G.; Li, Y.; Xu, Z. Rapid screening of SARS-CoV-2 inhibitors via ratiometric fluorescence of RBD-ACE2 complexes in living cells by competitive binding. *Acta Pharmaceutica Sinica B* **2022**, *12*, 3739−3742.
(29) Liu, X.; Qiao, Q.; Tian, W.; Liu, W.; Chen, J.; Lang, M. J.; Xu, Z. Aziridinyl Fluorophores Demonstrate Bright Fluorescence and Superior Photostability by Effectively Inhibiting Twisted Intramolecular Charge Transfer. *J. Am. Chem. Soc.* **2016**, *138*, 6960−6963.
(30) Grimm, J. B.; English, B. P.; Chen, J.; Slaughter, J. P.; Zhang, Z.; Revyakin, A.; Patel, R.; Macklin, J. J.; Normanno, D.; Singer, R. H.; Lionnet, T.; Lavis, L. D. A general method to improve fluorophores for live-cell and single-molecule microscopy. *Nat. Methods* **2015**, *12*, 244−250.
(31) Jing, C.; Cornish, V. W. Chemical Tags for Labeling Proteins Inside Living Cells. *Acc. Chem. Res.* **2011**, *44*, 784−792.
(32) Liu, W.; Chen, J.; Qiao, Q.; Liu, X.; Xu, Z. A TICS-fluorophore based probe for dual-color GSH imaging. *Chin. Chem. Lett.* **2022**, *33*, 4943−4947.
(33) Zhou, W.; Fang, X.; Qiao, Q.; Jiang, W.; Zhang, Y.; Xu, Z. Quantitative assessment of rhodamine spectra. *Chin. Chem. Lett.* **2021**, *32*, 943−946.
(34) Chen, J.; Liu, W.; Fang, X.; Qiao, Q.; Xu, Z. BODIPY 493 acts as a bright buffering fluorogenic probe for super-resolution imaging of lipid droplet dynamics. *Chin. Chem. Lett.* **2022**, *33*, 5042−5046.
(35) Zbinden, A.; Pérez-Berlanga, M.; De Rossi, P.; Polymenidou, M. Phase Separation and Neurodegenerative Diseases: A Disturbance in the Force. *Developmental Cell* **2020**, *55*, 45−68.
(36) Wolf, M.; Roosen-Runge, F.; Zhang, F.; Roth, R.; Skoda, M. W. A.; Jacobs, R. M. J.; Sztucki, M.; Schreiber, F. Effective interactions in protein-salt solutions approaching liquid-liquid phase separation. *J. Mol. Liq.* **2014**, *200*, 20−27.
(37) Burke, K. A.; Janke, A. M.; Rhine, C. L.; Fawzi, N. L. Residue-by-Residue View of In Vitro FUS Granules that Bind the C-Terminal Domain of RNA Polymerase II. *Mol. Cell* **2015**, *60*, 231−241.
(38) Boyko, S.; Qi, X.; Chen, T.-H.; Surewicz, K.; Surewicz, W. K. Liquid-liquid phase separation of tau protein: The crucial role of electrostatic interactions. *J. Biol. Chem.* **2019**, *294*, 11054−11059.
(39) Nott, T. J.; Petsalaki, E.; Farber, P.; Jervis, D.; Fussner, E.; Plochowietz, A.; Craggs, T. D.; Bazett-Jones, D. P.; Pawson, T.; Forman-Kay, J. D.; Baldwin, A. J. Phase Transition of a Disordered Nuage Protein Generates Environmentally Responsive Membraneless Organelles. *Mol. Cell* **2015**, *57*, 936−947.
(40) Moghaddam, S. Z.; Thormann, E. The Hofmeister series: Specific ion effects in aqueous polymer solutions. *J. Colloid Interface Sci.* **2019**, *555*, 615−635.
(41) Dormann, D.; Rodde, R.; Edbauer, D.; Bentmann, E.; Fischer, I.; Hruscha, A.; Than, M. E.; Mackenzie, I. R. A.; Capell, A.; Schmid, B.; Neumann, M.; Haass, C. *ALS-associated fused in sarcoma (FUS) mutations disrupt Transportin-mediated nuclear import* **2010**, *29*, 2841−2857.
(42) Gibb, C. L. D.; Gibb, B. C. Anion Binding to Hydrophobic Concavity Is Central to the Salting-in Effects of Hofmeister Chaotropes. *J. Am. Chem. Soc.* **2011**, *133*, 7344−7347.
(43) Parsons, D. F.; Boström, M.; Maceina, T. J.; Salis, A.; Ninham, B. W. Why Direct or Reversed Hofmeister Series? Interplay of Hydration, Non-electrostatic Potentials, and Ion Size. *Langmuir* **2010**, *26*, 3323−3328.
(44) Salis, A.; Ninham, B. W. Models and mechanisms of Hofmeister effects in electrolyte solutions, and colloid and protein systems revisited. *Chem. Soc. Rev.* **2014**, *43*, 7358−7377.
(45) De Marco, G.; Lomartire, A.; Manera, U.; Canosa, A.; Grassano, M.; Casale, F.; Fuda, G.; Salamone, P.; Rinaudo, M. T.; Colombatto, S.; Moglia, C.; Chiò, A.; Calvo, A. Effects of intracellular calcium accumulation on proteins encoded by the major genes underlying amyotrophic lateral sclerosis. *Sci. Rep.* **2022**, *12*, 395.
(46) Shepilov, M. P. Calculation of kinetics of metastable liquid-liquid phase separation for the model with simultaneous nucleation of particles. *J. Non-Cryst. Solids* **1992**, *146*, 1−25.

https://doi.org/10.1021/cbmi.3c00094
Chem. Biomed. Imaging 2024, 2, 70−80